


## ORIGINAL RESEARCH PAPER

# Magnetic core-shell $\text{Fe}_3\text{O}_4@\text{TiO}_2$ nanocomposites for broad spectrum antibacterial applications

Nisha Rani | Brijnandan S. Dehiya 

Department of (MSN) Materials Science and Nanotechnology, Deenbandhu Chhotu Ram University of Science and Technology (DCRUST), Murthal, Haryana, India

**Correspondence**

Brijnandan S. Dehiya, Department of (MSN) Materials Science and Nanotechnology, Deenbandhu Chhotu Ram University of Science and Technology (DCRUST), Murthal, Haryana, India.  
Email: [drbrijdehiya.msn@dcrustm.org](mailto:drbrijdehiya.msn@dcrustm.org)

**Abstract**

The authors have synthesised a core-shell  $\text{Fe}_3\text{O}_4@\text{TiO}_2$  nanocomposite consisting of  $\text{Fe}_3\text{O}_4$  as a magnetic core, and  $\text{TiO}_2$  as its external shell. The  $\text{TiO}_2$  shell is primarily intended for use as a biocompatible and antimicrobial carrier for drug delivery and possible other applications such as wastewater remediation purposes because of its known antibacterial and photocatalytic properties. The magnetic core enables quick and easy concentration and separation of nanoparticles. The magnetite nanoparticles were synthesized by a hydrothermal route using ferric chloride as a single-source precursor. The magnetite nanoparticles were then coated with titanium dioxide using titanium butoxide as a precursor. The core-shell  $\text{Fe}_3\text{O}_4@\text{TiO}_2$  nanostructure particles were characterized by XRD, UV spectroscopy, and FT-IR, TEM, and VSM techniques. The saturation magnetization of  $\text{Fe}_3\text{O}_4$  nanoparticles was significantly reduced from 74.2 to 13.7 emu/g after the  $\text{TiO}_2$  coating. The antibacterial studies of magnetic nanoparticles and the titania-coated magnetic nanocomposite were carried out against gram+ve, and gram-ve bacteria (*Staphylococcus aureus*, *Pseudomonas aeruginosa*, *Shigella flexneri*, *Escherichia coli*, and *Salmonella typhi*) using well diffusion technique. The inhibition zone for *E. coli* (17 mm after 24 h) was higher than the other bacterial strains; nevertheless, both the uncoated and  $\text{TiO}_2$ -coated magnetite nanocomposites showed admirable antibacterial activity against each of the above bacterial strains.

## 1 | INTRODUCTION

Metal oxide nanostructured particles are of great significance in the field of antibacterial studies because of large surface areas with extremely active sites. A very discrete type of binary-metal oxide having good magnetization and unique biocompatibility is magnetite ( $\text{Fe}_3\text{O}_4$ ) especially with crystal size on the nano-scale.  $\text{Fe}_3\text{O}_4$  nanoparticles have been widely used because of some of its excellent optical and magnetic properties [1–4]. In addition to these, plural cationic oxidation states in  $\text{Fe}_3\text{O}_4$  nanoparticles provide an extra edge over other materials for physicochemical applications [5–7]. Various methods have been used by researchers to synthesize high-quality monodisperse magnetic nanoparticles such as chemical coprecipitation, solvothermal, hydrothermal, microemulsion, thermolysis, decomposition of precursors, sol-gel, and polyol methods [8–16]. The agglomeration of crystals is an undesirable occurrence during the synthesis of magnetic nanoparticles. Functionalization and coating of nucleated crystals with ligands

can prevent the agglomeration of nanoparticles. Nanoparticles can also have a stronger interaction with the biological cells' surface because of their high surface area to volume ratio compared with bulkier crystals [17]. Some nanoparticles like ZnO, CdSe,  $\text{TiO}_2$ , ZnS, and  $\text{SiO}_2$  have shown considerable antibacterial/antimicrobial activity, and selective toxicity in biological systems has previously reported [18]. The antibacterial activity of  $\text{TiO}_2$  has been attributed mainly to its capability to activate free hydroxyl radicals ( $\text{OH}^\cdot$ ) under the action of sunlight/ultraviolet radiation [19].

Combining  $\text{Fe}_3\text{O}_4$  and  $\text{TiO}_2$  nanoparticles to achieve the easy recovery and recycling of  $\text{TiO}_2$  nanoparticles permits one solution of remediating the contamination of the environment by wastewater. The synthesized nanocomposites could also be easily removed using a magnet after antibacterial application allowing for repeated use of the nanomaterial. The biochemical interaction that occurs between the nanoparticles and the microbes has been attributed to the positive charge on nanoparticles and the negative charge on the outer cell walls of the microbes, which

This is an open access article under the terms of the Creative Commons Attribution License, which permits use, distribution and reproduction in any medium, provided the original work is properly cited.

© 2021 The Authors. *IET Nanobiotechnology* published by John Wiley & Sons Ltd on behalf of The Institution of Engineering and Technology.

results in the oxidation of microbes and quick death [20]. Cell lysis mechanism also involves the reaction between the ions generated by nanostructures particles and protein on the bacterial cell [21]. The mechanism of antibacterial action by the nanoparticles thus is also through the oxidative stress due to Reactive Oxygen Species (ROS) that are generated by the nanoparticles [22, 23]. The singlet oxygen produced could also damage the proteins or the DNA in the bacteria and thus lead to the bacteria's degradation. Kim et al. studied the generation of  $H_2O_2$  when  $Fe^{2+}$  reacted with dissolved oxygen. The reaction between the  $Fe^{2+}$  and  $H_2O_2$  also creates the  $\cdot OH$  radical, which harms the biological macromolecules' structures [24].

Magnetite ( $Fe_3O_4$ ) nanoparticles were prepared by using a single precursor. Afterwards, the magnetite nanoparticles were coated with titania using titanium butoxide as a precursor. We have explored here the effect of these  $Fe_3O_4@TiO_2$  nanostructured composite particles as antibacterial agents on five different pathogen bacteria such as *Staphylococcus aureus*, *Pseudomonas aeruginosa*, *Shigella flexneri*, *Escherichia coli*, and *Salmonella typhi*. A unique attraction for this study was that these nanocomposites can be quickly concentrated, recovered, and recycled using a simple magnetic separation technique, in-vitro and in-vivo.

## 2 | EXPERIMENTAL DESIGN

### 2.1 | Materials

Iron (III) chloride,  $NH_4Ac$ , ethylene glycol (EG), tetracycline, polyvinyl pyrrolidone, and LB agar were all purchased commercially (MERCK). Titanium butoxide was purchased from Sigma Aldrich. Five bacterial species, that is, *S. aureus*, *P. aeruginosa*, *Shigella flexneri*, *E. coli*, and *S. typhi*, were acquired locally from the Department of Biotechnology, DCRUST University, Sonapat, India.

### 2.2 | Synthesis route

#### 2.2.1 | Synthesis of $Fe_3O_4$ nanoparticles

0.6 M of Iron(III) chloride,  $NH_4Ac$  (1.5 M), and PVP (0.25 M) were put in 40 ml of ethylene glycol under magnetic stirring. After 3 h of mixing, the solution was shifted into an autoclave for hydrothermal action at  $200^\circ C$  for 20 h. Finally, the autoclave was cooled down, and the black precipitate was taken apart with a magnet. The precipitate was rinsed with ethanol and dehydrated at  $70^\circ C$  for 7–8 h [25].

#### 2.2.2 | Synthesis of $Fe_3O_4@TiO_2$ nanoparticles

0.5 g of  $Fe_3O_4$  nanostructure particles were put in 10 ml of ethanol with a concentrated 0.50 ml ammonia solution under ultrasound for 20 min. Afterwards, 5 ml of TBOT in ethanol (40 ml) was put into the solution drop wise under the stirrer.

Following 2 h stirring at room temperature, the ultrasonication was done for 2 h. The suspension was put into an autoclave for hydrothermal action at  $200^\circ C$  for 20 h. The sample was taken apart by a magnet, rinsed with ethanol, and dried at  $70^\circ C$ .

### 2.3 | Antibacterial activities screening using the well diffusion method

250 ml of LB agar was prepared. The media was poured into five Petri plates. Once the medium was solidified, 500  $\mu l$  of cultures of age 18–24 h were spread on solidified media in all Petri plates. Then uniform holes were made, and 50 mg/ml concentration of nanoparticles was poured into the holes. The enclosed parafilm plates were set aside into the incubator at  $37^\circ C$  for 24 h. A negative control (ethanol) and positive control (15  $\mu l$  of 10 mg/ml tetracycline) was used. The zone of inhibition was noted in mm [26].

## 3 | RESULTS AND DISCUSSION

### 3.1 | XRD characterisation

#### 3.1.1 | $Fe_3O_4$ nanoparticles

Figure 1 shows the X-ray diffraction pattern from the magnetite synthesized by the chemical co-precipitation process. These nanoparticles have been investigated using XRD. The XRD chart of magnetite nanostructure particles corresponds to a sequence of peaks at  $2\theta$  of  $30.1^\circ$ ,  $35.5^\circ$ ,  $43.2^\circ$ ,  $53.4^\circ$ ,  $57.2^\circ$ , and  $62.8^\circ$ , which are associated to the (220), (311), (400), (422), (511), and (440) planes of magnetite, respectively (Crystallography Open Database PDF No. 96-101-1085) [27].

The highly crystalline structure of the magnetite is shown by the sharp peaks of the XRD graph in Figure 1.

#### 3.1.2 | $Fe_3O_4@TiO_2$ nanoparticles

The XRD graph of these nanocomposites shows peaks at  $2\theta$  of  $25.3^\circ$ ,  $37.8^\circ$ ,  $48.2^\circ$ , that is corresponding to the reflection of (101), (104), and (200) planes of  $TiO_2$  nanostructures particles, respectively [28]. Some peaks of  $Fe_3O_4$  cores and the intense peaks of anatase form of titania are shown in the XRD graph, confirming the presence of  $TiO_2$  coating on magnetite nanostructured particles (Figure 2), which reduces the relative peak intensity of the magnetite phase in the diffraction pattern.

### 3.2 | FTIR

#### 3.2.1 | $Fe_3O_4$ nanoparticles

The FTIR spectrum represents hydroxyl group, which is recognized as absorption at  $3429\text{ cm}^{-1}$ . The band at  $2929\text{ cm}^{-1}$  can be attributed to the  $CH_2$  stretching bond.

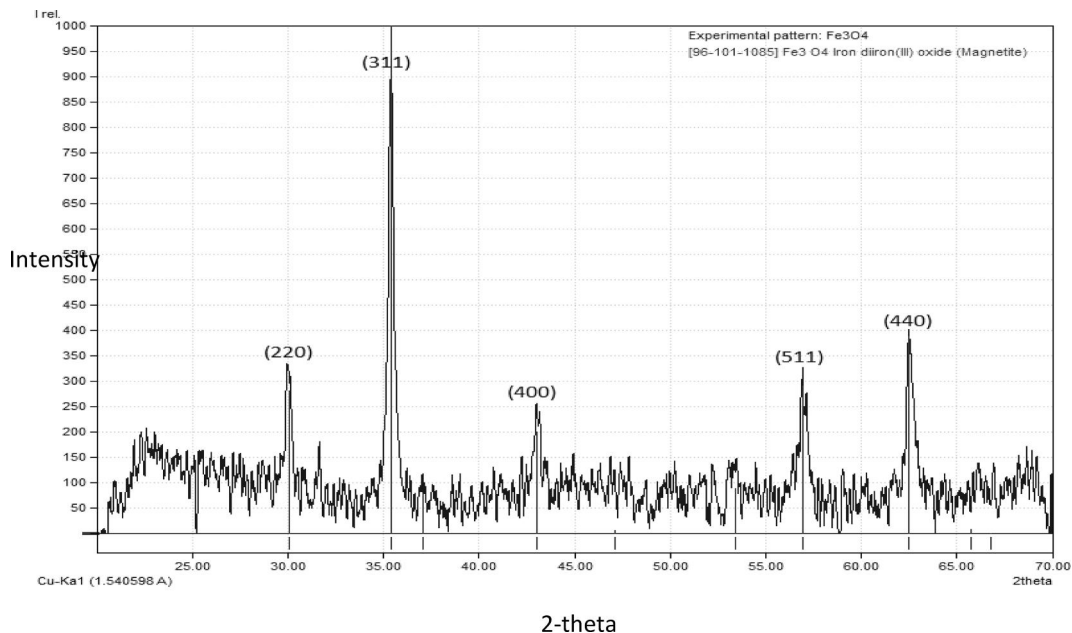


FIGURE 1 The X-ray diffraction graph of the chemically synthesized magnetite nanoparticles is shown

FIGURE 2 The X-ray diffraction graph of Fe<sub>3</sub>O<sub>4</sub>@TiO<sub>2</sub> core-shell nanocomposite is shown here

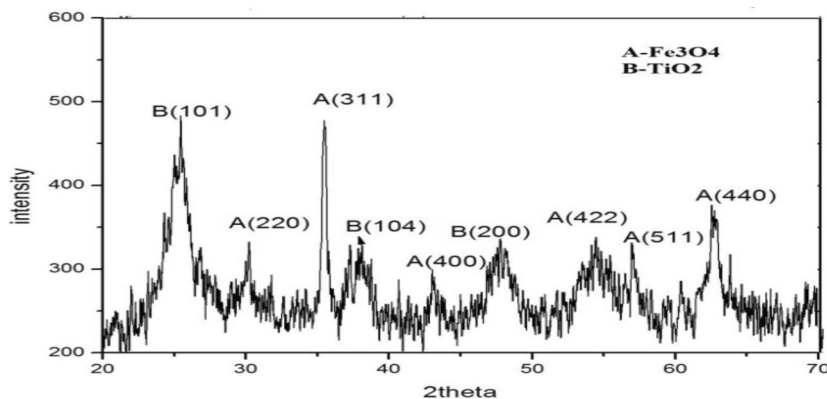
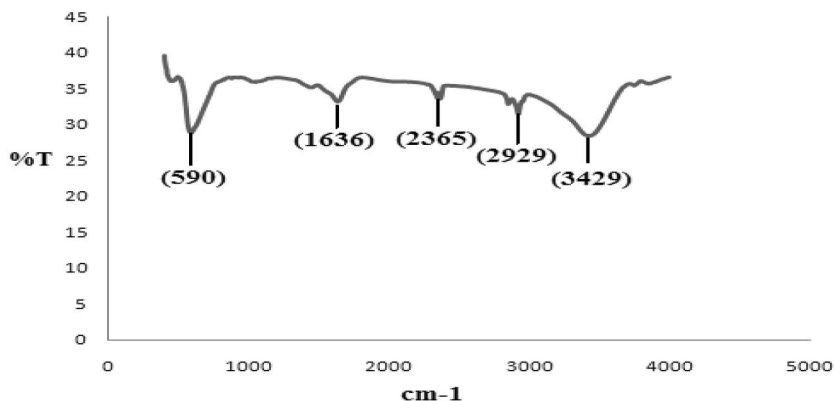
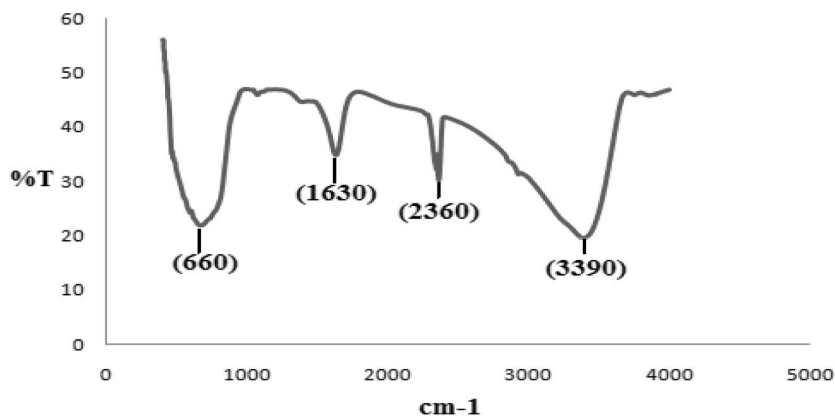
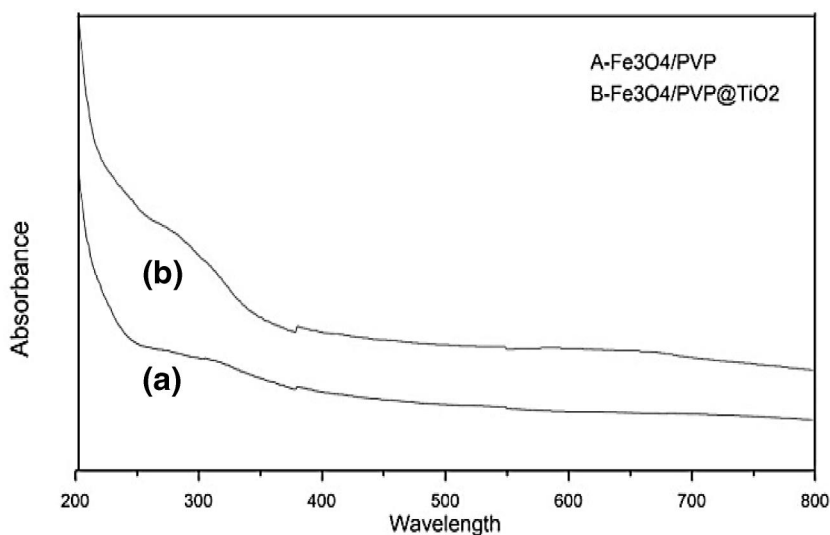


FIGURE 3 FTIR spectrum of the uncoated Fe<sub>3</sub>O<sub>4</sub> nanoparticles is shown here





**FIGURE 4** The FTIR spectrum of  $\text{Fe}_3\text{O}_4@\text{TiO}_2$  nanoparticles is shown here



**FIGURE 5** UV-Vis absorbance spectra of the uncoated  $\text{Fe}_3\text{O}_4$  nanoparticles (a) and of the  $\text{Fe}_3\text{O}_4@\text{TiO}_2$  nanocomposite (b)

The band at  $2365\text{ cm}^{-1}$  is due to  $\text{CO}_2$  in the atmosphere. In the spectrum, absorption at  $590\text{ cm}^{-1}$  shows a Fe-O bond. The peak at  $1636\text{ cm}^{-1}$  is reported as an amino group [29] (Figure 3).

### 3.2.2 | $\text{Fe}_3\text{O}_4@\text{TiO}_2$ nanoparticles

The FTIR spectrum showed a band at  $3390\text{ cm}^{-1}$ , which is recognized as an O-H bond. The band at  $2360\text{ cm}^{-1}$  is ascribed to the presence of  $\text{CO}_2$  in the chamber atmosphere.

The band at  $1630\text{ cm}^{-1}$  is recognized as NH bending. The band at  $660\text{ cm}^{-1}$  is assigned to the Ti-O-Ti stretching vibrations [30] (Figure 4).

### 3.3 | UV characterization

Figure 5 shows the absorption spectrum of magnetite and titania-coated  $\text{Fe}_3\text{O}_4$  nanocomposite. When titania nanoparticles were coated on the  $\text{Fe}_3\text{O}_4$  nanoparticles, the absorption peak(s) was shifted into the visible region.

### 3.4 | TEM characterization

Both single-phase  $\text{Fe}_3\text{O}_4$  nanoparticles and  $\text{Fe}_3\text{O}_4@\text{TiO}_2$  core-shell nanostructures, were synthesized using a single precursor by the hydrothermal process. A lot of nanostructured crystalline granules of titania appear to enclose a magnetite core. The titanium dioxide is present as the externally deposited film on the  $\text{Fe}_3\text{O}_4$  nanostructure particles, creating the  $\text{Fe}_3\text{O}_4@\text{TiO}_2$  nanostructure [31] (Figure 6).

### 3.5 | VSM characterization

The magnetic features of  $\text{Fe}_3\text{O}_4$  nanoparticles and  $\text{Fe}_3\text{O}_4@\text{TiO}_2$  nanostructure composites have been studied using the VSM technique (Figure 7).

The saturation magnetization ( $M_s$ ) of magnetite nanostructure particles and  $\text{Fe}_3\text{O}_4@\text{TiO}_2$  nanostructure composites were  $74.268\text{ emu/g}$  and  $13.755\text{ emu/g}$ , respectively. The saturation magnetization ( $M_s$ ) reduced because of the non-magnetic  $\text{TiO}_2$  outside film on nanoparticles (Table 1).

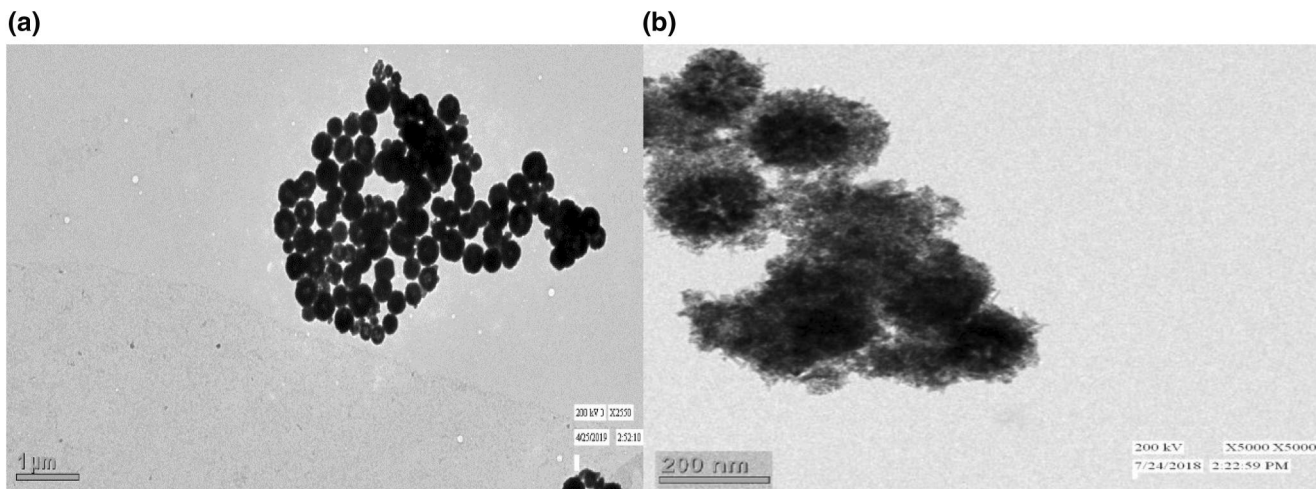


FIGURE 6 (a) TEM images of magnetite nanoparticles (b) TEM images of titania-coated magnetite nanocomposite structures

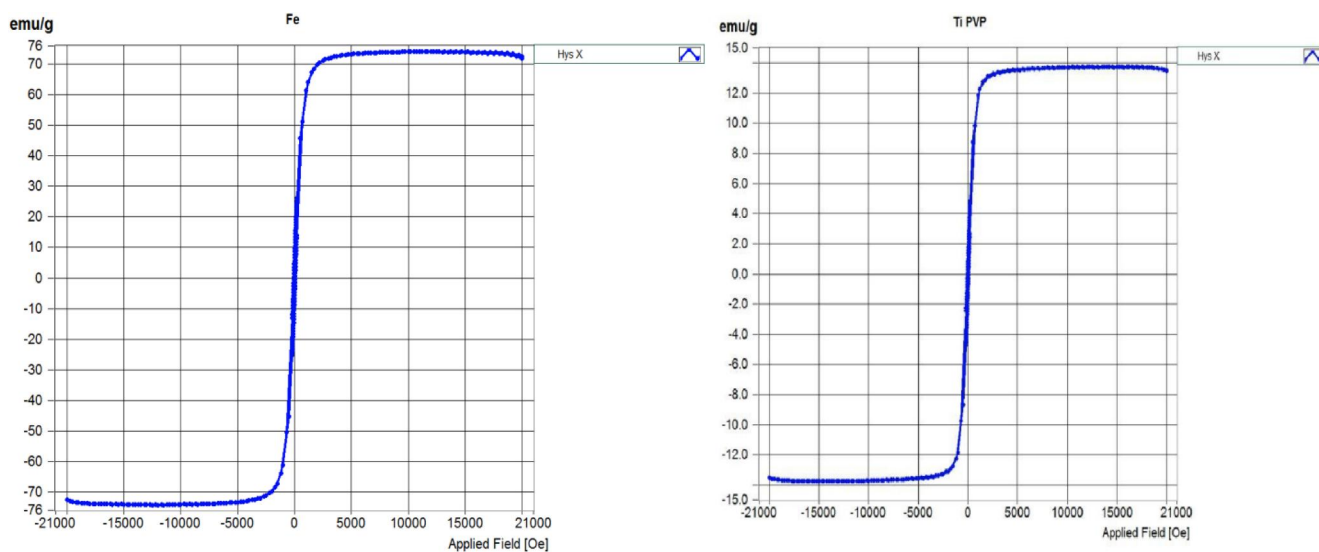


FIGURE 7 Saturation magnetization of magnetite and titania-coated magnetic nanoparticles

Photocatalytic actions of oxide nanoparticles

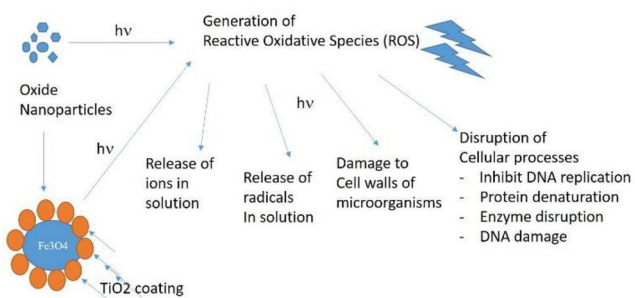


FIGURE 8 The mechanism of interaction of oxide NPs with bacterial/microbial cells

3.6 | Antibacterial activities

TiO<sub>2</sub>-coated magnetite exhibited bactericidal activity in resistance to both gram +ve (positive) and gram -ve (negative) bacteria. The antibacterial activity by the core-shell nanocomposite is likely due to the oxidative stress produced by reactive oxygen species (ROS) which include superoxide radical (O<sup>-2</sup>), hydroxyl radical (·OH), and also hydrogen peroxide (H<sub>2</sub>O<sub>2</sub>) (Figure 8). Collin [32] showed how hydrogen peroxide (H<sub>2</sub>O<sub>2</sub>) and other ROS were generated when Fe<sup>2+</sup>/Fe<sup>3+</sup> reacted with oxygen. The biochemical interaction occurs between H<sub>2</sub>O<sub>2</sub> and membrane proteins or between the substance formed due to magnetite nanoparticles and bacteria's external bilayer. Then H<sub>2</sub>O<sub>2</sub> enters the outer bilayer of bacteria and destroys them [33]. The various oxidation and reduction

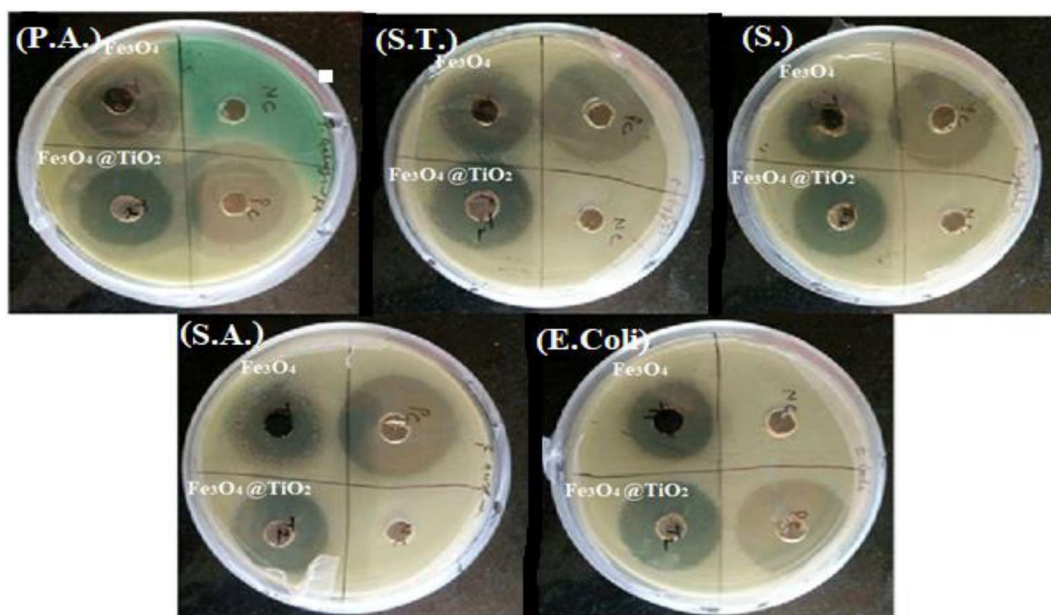


**TABLE 1** The magnetic measurements of the uncoated and TiO<sub>2</sub>-coated magnetite samples

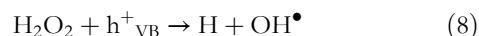
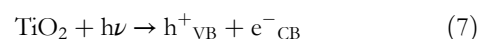
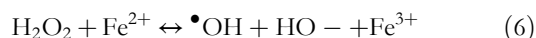
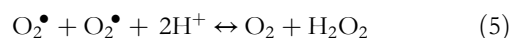
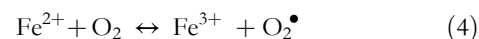
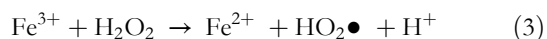
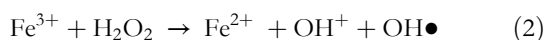
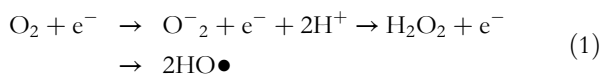
S. No.	Sample Name	Saturation Magnetization (M <sub>s</sub> ) (emu/g)	Coercivity (H <sub>c</sub> ) (Oe)	Remanence (M <sub>r</sub> ) (emu/g)
1	Fe <sub>3</sub> O <sub>4</sub> /PVP	74.268	69.217	7.120
2	Fe <sub>3</sub> O <sub>4</sub> /PVP@TiO <sub>2</sub>	13.755	69.366	1.316

**TABLE 2** The diameter of the inhibition zone for Fe<sub>3</sub>O<sub>4</sub>@TiO<sub>2</sub> nanocomposites against different extracts

S. No.	Strain	Inhibition Zone (mm) (Fe <sub>3</sub> O <sub>4</sub> )	Inhibition Zone (mm) (Fe <sub>3</sub> O <sub>4</sub> @TiO <sub>2</sub> )
1	<i>Staphylococcus aureus</i> (gram +)	13.33 ± 0.58	16.17 ± 0.29
2	<i>Escherichia coli</i> (gram -)	15.50 ± 0.50	16.50 ± 0.50
3	<i>Shigella flexneri</i> (gram -)	11.17 ± 0.76	14.83 ± 0.76
4	<i>Pseudomonas aeruginosa</i> (gram -)	10.50 ± 0.50	15.83 ± 0.29
5	<i>Salmonella typhi</i> (gram -)	12.67 ± 0.29	14.33 ± 0.76

**FIGURE 9** Antibacterial activity of both Fe<sub>3</sub>O<sub>4</sub> nanoparticles and Fe<sub>3</sub>O<sub>4</sub>@TiO<sub>2</sub> nanocomposites against different extracts, that is, P.A. – *P. aeruginosa*, S.T. – *S. typhi*, S. – *Shigella flexneri*, S.A. – *S. aureus*, *E. coli*

reactions occur when Fe<sub>3</sub>O<sub>4</sub>@TiO<sub>2</sub> nanocomposites disperse within the media, known as the Fenton reaction in case of the iron ionic species. These reactions generate different reactive oxygen species because of the Fe<sup>3+</sup> and Fe<sup>2+</sup> present in magnetite [34, 35]. It has also been reported that Fe<sup>3+</sup> doping of TiO<sub>2</sub> reduces agglomeration resulting in high photocatalytic efficiency and a reduced bandgap of about 2.6 eV [36]. Several oxidation-reduction and photocatalytic reactions can occur simultaneously in this combination:



OH<sup>•</sup> and HO<sub>2</sub><sup>•</sup> produced in the reaction are reactive free radicals. Magnetite (Fe<sub>3</sub>O<sub>4</sub>) NPs can slowly be oxidized to maghemite (γ-Fe<sub>2</sub>O<sub>3</sub>). This oxidation is a critical part of the origin of oxidative stress to the cell of bacteria, resulting in the bacterial cell's death.

Table 2 and figure 9 depict the effect of the uncoated and coated magnetite nanoparticles on the five different species of microorganisms. The terms 'nc' and 'pc' in Figure 9 refer to

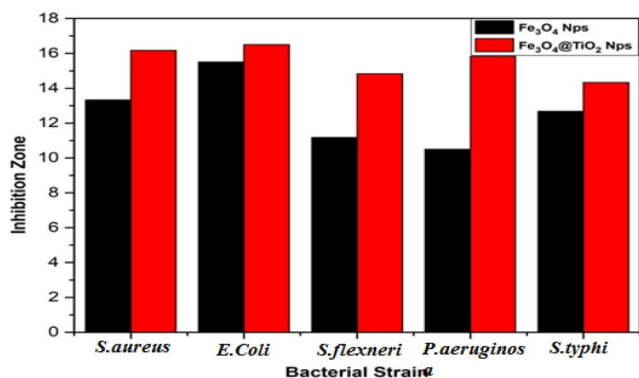


**FIGURE 10** Antibacterial index of magnetite nanoparticles and titania-coated magnetic nanocomposites are shown here

negative control and positive control, respectively. The antibacterial actions of both types of the nanoparticles are clearly very significant, with TiO<sub>2</sub>-coated particles providing superior antibacterial action. The strongest effect was observed on *E. coli* bacteria for both the types of nanomaterials.

### 3.6.1 | Antibacterial index of magnetite nanoparticles

The antibacterial index of magnetite nanostructures particles and Fe<sub>3</sub>O<sub>4</sub>@TiO<sub>2</sub> nanocomposite was shown in Figure 10. The Fe<sub>3</sub>O<sub>4</sub>@TiO<sub>2</sub> nanocomposite exhibited a better bactericidal activity for *E. coli* as compared with other bacterial strains.

The magnetite nanoparticles, as core materials, showed good bactericidal activity. The maximum antibacterial activity was observed for TiO<sub>2</sub>-coated nanoparticles because of its inherent antibacterial properties [37]. The core-shell Fe<sub>3</sub>O<sub>4</sub>@TiO<sub>2</sub> nanocomposite showed a better antibacterial effect than Fe<sub>3</sub>O<sub>4</sub> nanoparticles. The activity of Fe<sub>3</sub>O<sub>4</sub> nanoparticles to inactivate bacterial strains was improved significantly after coating with TiO<sub>2</sub>.

The core-shell Fe<sub>3</sub>O<sub>4</sub>@TiO<sub>2</sub> nanocomposite could be used for drug delivery because of the inherent antibacterial property of TiO<sub>2</sub> and the magnetic property of magnetite nanoparticles. The ability to kill cancer cells has also been previously studied [38, 39]. The TiO<sub>2</sub> nanoparticles have the capability to both oxidize the pollutants and kill the microorganisms [40]. The antibacterial effect of core-shell Fe<sub>3</sub>O<sub>4</sub>@TiO<sub>2</sub> nanocomposite was studied, which combined the treatment of microbial contamination and magnetic separation property of magnetite, synthesized. The antibacterial activity of TiO<sub>2</sub> nanoparticles using as a shell was better than that reported in previous studies [41, 42].

## 4 | CONCLUSION

Magnetite superparamagnetic nanostructures particles were fabricated using a single precursor by the hydrothermal

method and by using a reducing agent. The Fe<sub>3</sub>O<sub>4</sub> nanostructured particles were coated with titania using a separate hydrothermal process. The effect of the TiO<sub>2</sub> shell in the core-shell Fe<sub>3</sub>O<sub>4</sub>@TiO<sub>2</sub> nanocomposite as a broad-spectrum antibacterial agent was investigated, in comparison to the similar effect of the uncoated core magnetite itself. The antibacterial effects of magnetite core and the titania shell were studied on five bacteria strains: *S. aureus*, *P. aeruginosa*, *Shigella flexneri*, *E. coli*, and *S. typhi*. The Fe<sub>3</sub>O<sub>4</sub>@TiO<sub>2</sub> nanocomposites showed superior antibacterial action on each bacterium, while the uncoated magnetite's effect was significantly lesser in comparison. The TiO<sub>2</sub>-coated magnetite nanoparticles revealed better and more effective antibacterial activity against the *E. coli* strain of bacteria than the other strains. It can be concluded that Fe<sub>3</sub>O<sub>4</sub>@TiO<sub>2</sub> is a very active antibacterial agent, as verified by the large diameter of the inhibition zone. The results indicated that nanocomposites synthesized in this work could also be suitable materials for drug delivery applications. These can also be practical and cost-effective agents in cleaning a microbe-polluted water environment where the magnetic core lends itself to easy recycling. The results reveal that bacterial illness could be treated by core-shell Fe<sub>3</sub>O<sub>4</sub>@TiO<sub>2</sub> nanostructure particles employing TiO<sub>2</sub> as a shell due to its inherent antibacterial properties. Fe<sub>3</sub>O<sub>4</sub>@TiO<sub>2</sub> nanocomposites could be efficient and recyclable antibacterial agents because of their magnetic, anti-bacterial and photocatalytic features.

## ACKNOWLEDGEMENTS

The authors thank Dr. Pragati Jamdagni and Professor J.S. Rana, Dept of Biotechnology, DCRUST, for their invaluable support and supply of bacterial cultures for this study.

## ORCID

Brijnandan S. Dehiya  <https://orcid.org/0000-0002-6146-5966>

## REFERENCES

- Kim, Y.S., Kim, Y.H.: Application of ferro-cobalt magnetic fluid for oil sealing. *J. Magn. Mater.* 267, 105–110 (2003)
- Raj, K., Moskowitz, R.: A review of damping applications of ferrofluids. *Trans. Magn.* 16, 358–363 (2002)
- Beydoun, D., et al.: Novel photocatalyst: titania-coated magnetite. Activity and photodissolution. *J. Phys. Chem. B.* 104, 4387–4396 (2000)
- McMichael, R.D., et al.: Magnetocaloric effect in super paramagnets. *J. Magn. Mater.* 111, 29–33 (1992)
- Deng, Y., et al.: Synthesis of core/shell colloidal magnetic zeolite microspheres for the immobilization of trypsin. *Adv. Mater.* 21, 1377–1382 (2009)
- Xu, X., et al.: Synthesis of magnetic microspheres with immobilised metal ions for enrichment and direct determination of phosphopeptides by matrix-assisted laser desorption ionization mass spectrometry. *Adv. Mater.* 18, 32893293 (2006)
- Wang, Z., et al.: Facile synthesis of superparamagnetic fluorescent Fe<sub>3</sub>O<sub>4</sub>/ZnS hollow nanospheres. *J. Am. Chem. Soc.* 131, 11276–11277 (2009)
- Nabiyouni, G., et al.: Room temperature synthesis and magnetic property studies of Fe<sub>3</sub>O<sub>4</sub> nanoparticles prepared by a simple precipitation method. *J. Ind. Eng. Chem.* 21, 599–603 (2015)

9. Shaker, S., et al.: Preparation and characterization of magnetite nanoparticles by sol-gel method for water treatment. *Int. J. Inn. Res. Sci. Eng. Technol.* 2, 2969–2973 (2013)
10. Davarpanah, S.J., Karimian, R., Piri, F.: Synthesis of copper (II) oxide (CuO) nanoparticles and its application as gas sensors. *Appl. Biotechnol. Rep.* 2, 329–332 (2015)
11. Song, W., et al.: Water-soluble polyacrylamide coated-Fe<sub>3</sub>O<sub>4</sub> magnetic composites for high-efficient enrichment of U(VI) from radioactive wastewater. *Chem. Eng. J.* 246, 268–272 (2014)
12. Ankamwar, B., et al.: Biocompatibility of Fe<sub>3</sub>O<sub>4</sub> nanoparticles evaluated by in vitro cytotoxicity assays using normal, glia and breast cancer cells. *Nanotechnol.* 9, 075102–075110 (2010)
13. Tartaj, P., et al.: The preparation of magnetic nanoparticles for applications in biomedicine. *J. Phys. D Appl. Phys.* 36, R182R197 (2003)
14. Huang, H.S., Hainfeld, J.F.: Intravenous magnetic nanoparticle cancer hyperthermia. *Int. J. Nanomed.* 8, 2521–2532 (2013)
15. Martirosyan, K.S.: Thermosensitive magnetic nanoparticles for self-controlled hyperthermia cancer treatment. *J. Nanomed. Nanotechnol.* 3, e112-3 (2012)
16. Wu, W., et al.: Recent progress on magnetic iron oxide nanoparticles: synthesis, surface functional strategies, and biomedical applications. *Sci. Technol. Adv. Mater.* 16, 023501–023543 (2015)
17. Rizwan, W., et al.: Antibacterial activity of ZnO nanoparticles prepared via the non-hydrolytic solution route. *J. Appl. Microbiol. Biotechnol.* 87, 1917–1925 (2010)
18. Sobha, K., et al.: Emerging trends in nanobiotechnology. *J. Biotech. Mol. Bio. Rev.* 5, 001–012 (2010)
19. Gutierrez, F.M., et al.: Synthesis, characterization, and evaluation of the antimicrobial and cytotoxic effect of silver and titanium nanoparticles. *Nanomed.* 6, 681–688 (2010)
20. Rezaei-Zarchi, S., et al.: Comparative study of antimicrobial activities of TiO<sub>2</sub> and CdO nanoparticles against the pathogenic strain of *Escherichia coli*. *Iran J. Pathol.* 5, 83–89 (2010)
21. Zhang, H., Chen, G.: Potent antibacterial activities of Ag/TiO<sub>2</sub> nanocomposite powders synthesized by a one-pot sol-gel method. *Environ. Sci. Technol.* 43, 2905–2910 (2009)
22. Mahdy, S.A., Rasheed, Q.J., Kalaichelvan, P.T.: Antimicrobial activity of zero-valent iron nanoparticles. *Int. J. Mod. Eng. Res.* 2, 578–581 (2012)
23. Tran, N., et al.: Bactericidal effect of iron oxide nanoparticles on *Staphylococcus aureus*. *Int. J. Nanomed.* 5, 277–283 (2010)
24. Touati, D.: Iron and oxidative stress in bacteria. *Arch. Biochem. Biophys.* 373, 1–6 (2000)
25. Yang, Q., et al.: Preparation of magnetic Fe<sub>3</sub>O<sub>4</sub> microspheres using different surfactant and silica-coated magnetic particles. *AASRI International Conference on Industrial Electronics and Applications* (2015)
26. Chung, K.T., et al.: Effects of benzidine and benzidine analogs on the growth of bacteria, including *Azotobacter vinelandii*. *Environ. Toxicol. Chem.* 17, 271–275 (1998)
27. Hasanpour, A., Niyafar, M., Amighian, M.H.J.: A novel non-thermal process of TiO<sub>2</sub>-shell coating on Fe<sub>3</sub>O<sub>4</sub>-core nanoparticles. *J. Phys. Chem. Solid.* 73, 1066–1070 (2012)
28. Stefan, M., et al.: Synthesis and characterization of Fe<sub>3</sub>O<sub>4</sub>-TiO<sub>2</sub> core-shell nanoparticles. *J. Appl. Phys.* 116, 114312 (2014)
29. Mazario, E., et al.: Functionalization of iron oxide nanoparticles with HSA protein for thermal therapy. *IEEE Trans. Mang.* 0018–9464 (2016)
30. Abbasa, M., et al.: Fe<sub>3</sub>O<sub>4</sub>/TiO<sub>2</sub> core/shell nanocubes: single batch surfactant less synthesis, characterization, and efficient catalysts form methylene blue degradation. *Ceram. Int.* 40, 11177–11186 (2014)
31. Shen, X., et al.: Preparation and optical properties of TiO<sub>2-x</sub>N<sub>x</sub>/Ni<sub>0.5</sub>Zn<sub>0.5</sub>Fe<sub>2</sub>O<sub>4</sub> core-shell nanocatalyst from sol-gel-hydrothermal process. *J. Sol. Gel. Sci. Technol.* 54, 340–346 (2010). <https://doi.org/10.1007/s10971-010-2201-1>
32. Collin, F.: Chemical basis of reactive oxygen species reactivity and involvement in neurodegenerative diseases. *Int. J. Mol. Sci.* 20, 2407 (2019)
33. Padmavathy, N., Vijayaraghavan, R.: Enhanced bioactivity of ZnO nanoparticles—an antimicrobial study. *Sci. Technol. Adv. Mat.* 9, 35004–35010 (2008)
34. Kumar, S.R., Imlay, J.A.: How *Escherichia coli* tolerates profuse hydrogen peroxide formation by a catabolic pathway. *J. Bacteriol.* 195, 4569–4579 (2013)
35. Auffan, M., et al.: Chemical stability of metallic nanoparticles: a parameter is controlling their potential cellular toxicity in vitro. *Environ. Pollut.* 157, 1127–1133 (2009)
36. Zhou, M., Yu, J., Cheng, B.: Effects of Fe-doping on the photocatalytic activity of mesoporous TiO<sub>2</sub> powders prepared by an ultrasonic method. *J. Hazard Mater.* 137(3), 1838–1847 (2006). <https://doi.org/10.1016/j.jhazmat.2006.05.028>
37. Xinga, Y., et al.: Effect of TiO<sub>2</sub> nanoparticles on the antibacterial and physical properties of the polyethylene-based film. *Prog. Org. Coating.* 73, 219–224 (2012)
38. Blake, D.M., et al.: Application of the photocatalytic chemistry of titanium dioxide to disinfection and the killing of cancer cells. *Sep. Purif. Methods.* 28, 1–50 (1999)
39. Fujishima, A., Rao, T.N., Tryk, D.A.: Titanium dioxide photocatalysis. *J. Photochem. Photobiol. A C.* 1, 1–21 (2000)
40. Howard, A., et al.: Photocatalytic disinfection using titanium dioxide: spectrum and mechanism of antimicrobial activity. *Appl. Microbiol. Biotechnol.* 90, 1847–1868 (2011)
41. Morteza Haghi, M., et al.: Antibacterial effect of TiO<sub>2</sub> nanoparticles on the pathogenic strain of *E. coli*. *Int. J. Adv. Biotechnol. Res.* 3, 621–624 (2012)
42. Sodagar, A., et al.: Effect of TiO<sub>2</sub> nanoparticles incorporation on antibacterial properties and shear bond strength of dental composite used in orthodontics. *Dental Press. J. Orthod.* 22, 67–74 (2017)

**How to cite this article:** Rani N, Dehiya BS. Magnetic core-shell Fe<sub>3</sub>O<sub>4</sub>@TiO<sub>2</sub> nanocomposites for broad spectrum antibacterial applications. *IET Nanobiotechnol.* 2021;15:301–308. <https://doi.org/10.1049/nbt.12017>